

## Evolution from a Nodeless Gap to $d_{x^2-y^2}$ -Wave in Underdoped $\text{La}_{2-x}\text{Sr}_x\text{CuO}_4$

E. Razzoli,<sup>1</sup> G. Drachuck,<sup>2</sup> A. Keren,<sup>2</sup> M. Radovic,<sup>1,3</sup> N. C. Plumb,<sup>1</sup> J. Chang,<sup>1,3</sup>  
Y.-B. Huang,<sup>4</sup> H. Ding,<sup>4</sup> J. Mesot,<sup>1,3</sup> and M. Shi<sup>1</sup>

<sup>1</sup>Swiss Light Source, Paul Scherrer Institute, CH-5232 Villigen PSI, Switzerland

<sup>2</sup>Department of Physics, Technion, Haifa 32000, Israel

<sup>3</sup>Institut de la Matière Complexe, EPF Lausanne, CH-1015 Lausanne, Switzerland

<sup>4</sup>Beijing National Laboratory for Condensed Matter Physics, and Institute of Physics, Chinese Academy of Sciences, Beijing 100190, China  
(Received 9 June 2012; published 25 January 2013)

Using angle-resolved photoemission spectroscopy (ARPES), it is revealed that the low-energy electronic excitation spectra of highly underdoped superconducting and nonsuperconducting  $\text{La}_{2-x}\text{Sr}_x\text{CuO}_4$  cuprates are gapped along the entire underlying Fermi surface at low temperatures. We show how the gap function evolves to a  $d_{x^2-y^2}$  form with increasing temperature or doping, consistent with the vast majority of ARPES studies of cuprates. Our results provide essential information for uncovering the symmetry of the order parameter(s) in strongly underdoped cuprates, which is a prerequisite for understanding the pairing mechanism and how superconductivity emerges from a Mott insulator.

DOI: [10.1103/PhysRevLett.110.047004](https://doi.org/10.1103/PhysRevLett.110.047004)

PACS numbers: 74.72.Gh, 74.25.Jb, 79.60.Bm

In the BCS theory of superconductivity, the symmetry of the superconducting gap reflects the order parameter of the superfluid state and is directly tied to the symmetry of the interactions driving the formation of Cooper pairs. Similarly, other ordered phases, such as charge- or spin-density wave states, can induce gaps whose symmetries are connected to the underlying order parameters. Thus, in high-temperature superconductors, where superconductivity is found in close proximity to magnetic and charge order, the symmetry of the gap function is of critical theoretical importance. It is now widely accepted that the superconducting gap in moderately hole-doped high-temperature superconducting copper oxides (cuprates) exhibits a node located along the diagonal  $(0, 0)$ - $(\pi, \pi)$  line of the Brillouin zone (BZ), consistent with an overall gap function of pure  $d_{x^2-y^2}$  symmetry [1,2]. A key issue is whether  $d_{x^2-y^2}$  is the only form of the gap function for all cuprates over the full range of dopings. Using angle-resolved photoemission spectroscopy (ARPES), we reveal that the low-energy electronic excitation spectra of highly underdoped superconducting and nonsuperconducting  $\text{La}_{2-x}\text{Sr}_x\text{CuO}_4$  (LSCO) are gapped along the entire underlying Fermi surface (FS) at low temperatures. On the zone diagonal, gapless excitations appear as the temperature and/or doping is increased, and the gap function evolves to a  $d_{x^2-y^2}$  form.

ARPES experiments were carried out at the Surface and Interface Spectroscopy beam line at the Swiss Light Source on high-quality single crystals of LSCO, grown using the traveling solvent floating zone method. Circularly polarized light with  $h\nu = 55$  eV was used. Samples were cleaved *in situ* by using a specially designed cleaver [3]. The spectra were recorded with a VG Scienta R4000 electron analyzer. Because of the low

photoemission cross section of LSCO, energy resolution of  $\sim 14$ – $17$  meV was used to obtain a high photon flux for most measurements. Particular care was taken to avoid any electrostatic charging. No change in energy gap was observed when the photon flux was reduced by an order magnitude and the energy resolution was improved to  $\sim 10$  meV.

In Figs. 1(a)–1(d) we show ARPES spectra below and above the superconducting transition temperature ( $T_c$ ) for highly underdoped superconducting LSCO ( $x = 0.08$ ,  $T_c = 20$  K) along the diagonal line of the BZ. The spectra were obtained by deconvoluting the raw ARPES data to remove the broadening due to the finite instrumental resolution and then dividing the deconvoluted spectra by a Fermi distribution function [deconvolution-Fermi function division (DFD) method] [4]. Relative to  $E_F$ , a gap is clearly observed both below  $T_c$  (10 K) and above  $T_c$  (54 K). The gap closes above  $\sim 88$  K. To reveal the details of the gap, we trace the dispersion in the vicinity of  $E_F$ . In Figs. 1(e)–1(h) we plot energy distribution curves (EDCs) from Figs. 1(a)–1(d) along the zone diagonal cut. At low temperatures (10 and 54 K), moving from  $(0, 0)$  to  $(\pi, \pi)$ , the peak position of the EDCs approaches  $E_F$ , but before reaching  $E_F$ , it recedes to higher binding energies [Figs. 1(e) and 1(f)]. The spectral peak reaches  $E_F$  at 88 K [Fig. 1(g)] and crosses  $E_F$  at high temperatures [Fig. 1(h)], signaling the closure of the gap. In Figs. 1(i) and 1(j) the dispersion bending back below  $E_F$  at 10 K and crossing  $E_F$  at 137 K is better visualized by normalizing each EDC to its peak intensity.

In contrast to the observation of an energy gap along  $(0, 0)$ - $(\pi, \pi)$  at low temperatures for LSCO ( $x = 0.08$ ), we did not find such a gap in the spectra of the optimally doped sample ( $x = 0.145$ ,  $T_c = 33$  K). The dispersion in this

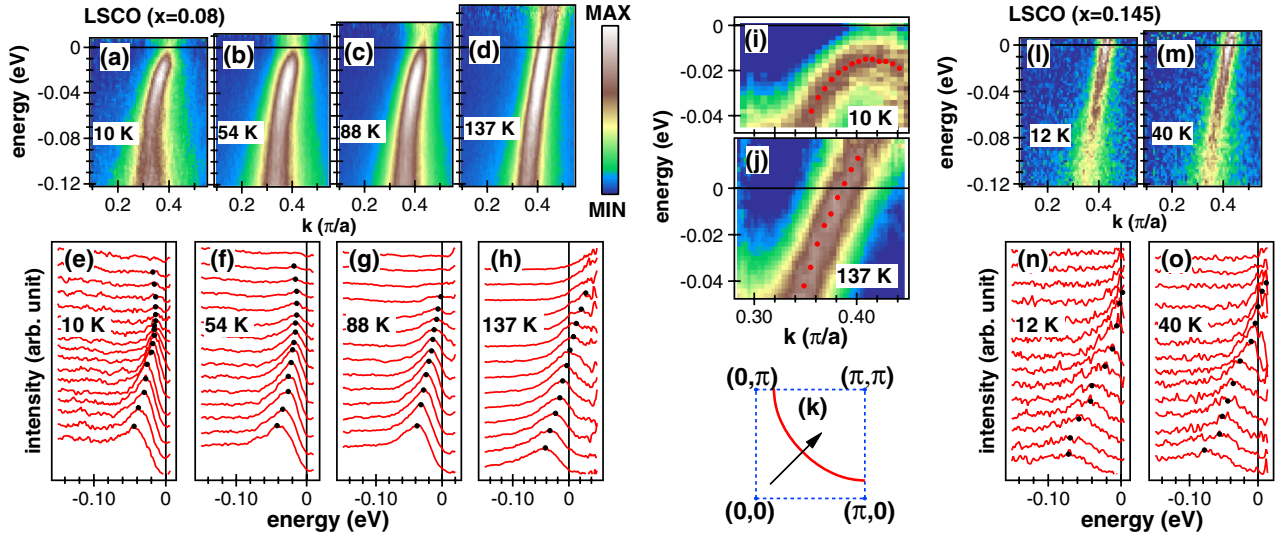


FIG. 1 (color online). ARPES spectra for LSCO with  $x = 0.08$  ( $T_c = 20$  K) and  $x = 0.145$  ( $T_c = 33$  K). (a)–(d) Intensities along the zone diagonal [the arrow in (k)] at  $T = 10, 54, 88,$  and  $137$  K for  $x = 0.08$ . The spectra were obtained by the DFD method [4]. (e)–(h) EDCs from (a)–(d) in the vicinity of  $k_F$ . (i), (j) Images in the vicinity of  $k_F$  at 10 and 137 K. Each EDC is normalized to the intensity at the peak position (circles). (k) The FS of LSCO  $x = 0.08$  obtained from tight-binding fits to the experimental data. The arrow indicates the cut along which the ARPES data were taken. (l), (m) The same as (a)–(d) but for LSCO ( $x = 0.145$ ) at  $T = 12$  and 40 K. (n), (o) EDCs from (l), (m) close to  $k_F$ .

higher hole-doped sample crosses smoothly through  $E_F$ , even at temperatures down to 12 K [Figs. 1(l)–1(o)].

A general observation in cuprates is that when  $T_c$  is crossed by decreasing the temperature, EDC peaks near the Fermi momentum ( $k_F$ ) along an off-nodal cut sharpen. This behavior was also observed in our ARPES spectra for LSCO ( $x = 0.08$ ) along the diagonal cut [the arrow in Fig. 1(k)]. In Figs. 2(a) and 2(b) we plot the EDCs at the  $k_F$  on the zone diagonal line as a function of temperature. The EDC peak width at 10 K ( $< T_c$ ) is considerably smaller than when the spectrum is measured above  $T_c$  ( $T = 54$  K) [Fig. 2(b)]. At low temperature (10 K) the peak width of the superconducting sample LSCO ( $x = 0.08$ ) is also smaller than that of the non-superconducting sample ( $x = 0.03$ ) [Fig. 2(b)], which indicates the change in the peak width is associated with the superconducting transition. To gain more insight about the differences between the spectra in the superconducting and nonsuperconducting phases, Figs. 2(c) and 2(d) show the EDCs as a function of doping at 10 K. The EDC peak positions of the  $x = 0.03$  and 0.08 samples occur at higher binding energy than in the  $x = 0.105$  and 0.145 samples [Fig. 2(c)], in which a simple  $d_{x^2-y^2}$  superconducting gap was observed [5,6]. For the superconducting samples, after aligning the peaks to the same position, the falling edges of the EDC peaks are almost identical at low binding energies [Fig. 2(d)], which demonstrates that the coherent peaks have a similar width in the superconducting state, and these widths are always significantly smaller than that of the nonsuperconducting sample.

The momentum dependence of the gap as a function of temperature is shown in Fig. 3. The measured raw EDCs at

$k_F$  were symmetrized to remove the effects of the Fermi function [7]. In the superconducting state, the extracted gap sizes were defined as half the peak-to-peak separation of the symmetrized EDCs. Above  $T_c$ , for those spectra having no coherent peak, the gap was defined as half the distance between the two locations where the slope has the largest change, as indicated by vertical lines in Fig. 3(c). For LSCO ( $x = 0.08$ ), the energy gap is highly anisotropic [Fig. 3(e)]. It has a maximal value at the zone boundary ( $\phi = 0^\circ$ ) and decreases monotonically along the FS to a minimum at the zone diagonal ( $\phi = 45^\circ$ ).

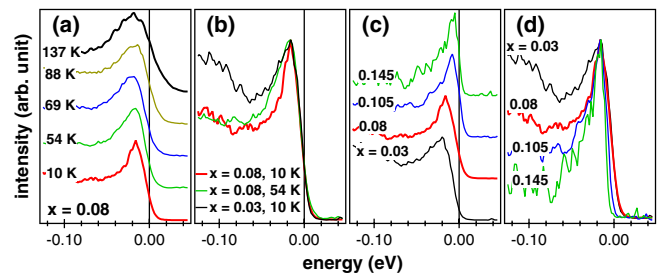


FIG. 2 (color online). EDCs at  $k_F$  on the zone diagonal for LSCO. The EDCs were obtained by deconvoluting the raw ARPES data to remove the broadening due to the finite instrumental resolution [4]. (a) EDCs as a function of temperature for  $x = 0.08$ . Curves are offset vertically for clarity. (b) EDCs for  $x = 0.03$  at 10 K, and for  $x = 0.08$  at 10 and 54 K. Curves are offset horizontally to align the peak position to that of the EDC for  $x = 0.08$  at 10 K. (c), (d) EDCs at 10 K as a function of doping ( $x$ ). Curves in (c) are offset vertically for clarity and in (d) are offset horizontally to align the peak position to that of the EDC for  $x = 0.08$  at 10 K.

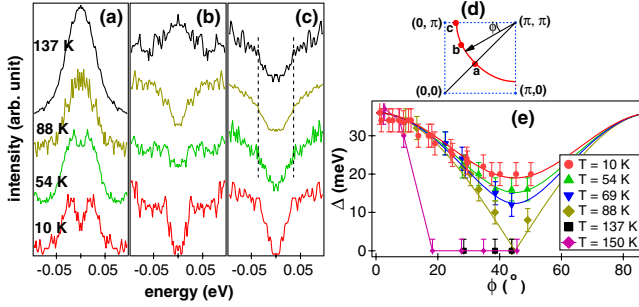


FIG. 3 (color online). ARPES spectra for LSCO ( $x = 0.08$ ). (a)–(c) Symmetrized EDCs as a function of temperature at  $k_F$  [points **a**, **b**, and **c** shown in (d)]. (d) The  $k_F$  (closed circles) at which the symmetrized EDCs are shown in (a)–(c). (e) Energy gap as a function of FS angle  $\phi$ . The symbols are the experimentally determined energy gaps at various temperatures. The solid lines are  $|\Delta_{d_{x^2-y^2}} + i\Delta_{d_{xy}}|$  with  $\Delta_{d_{x^2-y^2}}^0 = 38.52$  meV and from top to bottom  $\Delta_{d_{xy}}^0 = 20, 16.6, 13.5,$  and  $0$  meV (pure  $d_{x^2-y^2}$ -form), respectively.

However, at low temperatures, the gap function ( $\Delta$ ) strongly deviates from a pure  $d_{x^2-y^2}$  form,  $\Delta_{d_{x^2-y^2}}(\mathbf{k}) = \Delta_{d_{x^2-y^2}}^0 [\cos(k_x a) - \cos(k_y a)]/2$ , where  $a$  is the lattice constant. Below  $T_c$  at the  $k_F$  on the zone diagonal, a finite gap (hereafter we use the term “diagonal gap” for simplicity) is observed, which has an amplitude of  $\sim 20$  meV. As the temperature is increased, the diagonal gap monotonically decreases. It disappears at  $\sim 88$  K, at which point the gap function is very close to a pure  $d_{x^2-y^2}$  form [Fig. 3(e)]. At higher temperatures, gapless excitations appear on a portion of the FS centered at the zone diagonal (Fermi arc) and the arc length increases with temperature, a phenomenon that has been observed in early ARPES work of underdoped  $\text{Bi}_2\text{Sr}_2\text{CaCu}_2\text{O}_{8+\delta}$  [8] and other cuprates. In contrast to the temperature dependence of the diagonal gap, the gap size near the BZ boundary is insensitive to temperature in the range of 10 to 150 K; it always has a value of  $\sim 36$  meV [Fig. 3(e)].

The gap function obtained from the symmetrization method is confirmed with an independent procedure. We have applied the DFD method to high-statistics ARPES spectra [Figs. 4(a)–4(f)] along some selected cuts [Fig. 4(h)] to trace the dispersion in the vicinity of  $E_F$ . The energy gap was determined from the difference between  $E_F$  and the maximal energy that a backbending dispersion reaches [Fig. 4(g)]. Figure 4(i) shows the results of such an analysis applied to the data taken at 54 K. Within the error bars, the obtained gap function is consistent with that derived from the symmetrization method.

We note that the gap function of lightly doped LSCO has been studied by ARPES using the leading edge midpoints (LEM) on EDCs at  $k_F$  by Yoshida *et al.* [9], who did not report a diagonal gap. However, it is now well established that the LEM can give erroneous results, especially when

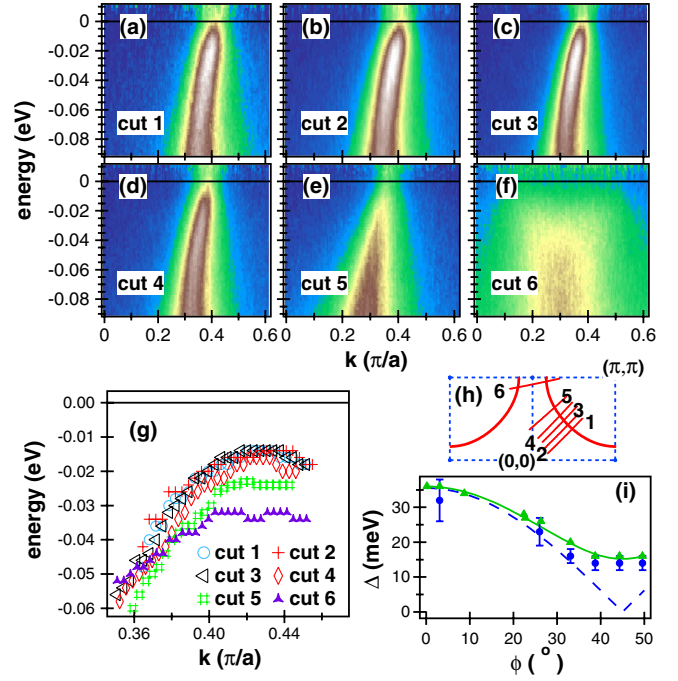


FIG. 4 (color online). ARPES spectra of LSCO ( $x = 0.08$ ,  $T_c = 20$  K) measured at 54 K. (a)–(f) Intensities along 6 cuts indicated in (h). The spectra were obtained by the DFD method. (g) Dispersions obtained by tracing the EDC peaks of (a)–(f) in the vicinity of  $k_F$ . For clarity the dispersions along cuts 2–6 were offset horizontally. (h) The upper half of BZ and cuts along which the data in (a)–(f) were taken. (i) Energy gap as a function of FS angle  $\phi$ . The closed circles are the gap extracted from the difference between  $E_F$  and the maximal energy that the backbending dispersions reach. The triangles are the gap obtained from symmetrized EDCs [Fig. 3(e)]. The dashed and solid lines are the  $|\Delta_{d_{x^2-y^2}}|$  and  $|\Delta_{d_{x^2-y^2}} + i\Delta_{d_{xy}}|$ , respectively.

the gap size is comparable to the resolution [10,11]. The EDC leading edge midpoint is indeed not a direct physical quantity, but instead results from a complicated combination of the gap size, the quasiparticle scattering rate, and the experimental resolution. In contrast to the LEM, within the BCS theory, the quasiparticle peak locations in the spectral function are set by  $\Delta(\mathbf{k})$  and thus tend to be far more robust against scattering and resolution effects [12]. Revisiting the previously published work, the quasiparticle peaks in the EDCs at  $k_F$  along the zone diagonal reported in Ref. [9] shift to higher binding energies as the doping is decreased (see. Fig. 1 in Ref [9]), consistent with the opening of a diagonal gap.

To explain our results, one natural line of thinking is to assume that both the superconducting gap and the pseudogap have  $d_{x^2-y^2}$  form, and the combination of disorder with long-range Coulomb interactions depresses the density of single-particle excitations at  $E_F$ , forming a so-called Coulomb gap [13,14]. A counterargument to this picture is that the scattering rate due to the disorder should drastically reduce the lifetime of the quasiparticles, which would

be manifested as severe broadening in the ARPES line shapes, essentially destroying the quasiparticle peak. By contrast, while there is a trend toward broader EDC line shapes with respect to decreasing doping [Fig. 2(d)], the quasiparticle peak is still clearly visible at the lowest doping, and a drastic crossover to Coulomb gap behavior is not observed.

One could instead consider a scenario in which an ordered phase (e.g., a spin-density wave) [15,16] or its fluctuations opens an energy gap along the entire FS in lightly doped LSCO ( $x < 0.105$ ). In such a picture, this phase is different from the superconducting instability, and below  $T_c$  it coexists with the superconducting phase, which has a  $d_{x^2-y^2}$  order parameter. The combination of these two order parameters would produce an energy gap on the entire FS. Recent Monte Carlo simulations have shown that a strong fluctuating competing order could open a diagonal gap in the superconducting phase, and a  $d_{x^2-y^2}$  gap function is restored with reduced amplitudes of the fluctuating competing order [17]. This scenario would explain why the diagonal gap is open in LSCO  $x = 0.08$  and  $0.03$  at low temperatures and is closed for  $x \geq 0.1$ , since it has been suggested that disordered magnetism is present at low doping and disappears at optimal doping [18,19]. In particular, strong indications of the presence of static or fluctuating spin-density wave ordering below optimal doping come from resistivity [20], heat transport [21], and neutron scattering measurements [22] at low temperatures. Nevertheless, it is not immediately clear how to reconcile our observations with the absence of a gap in optical conductivity data [23] or its expected signature in resistivity measurements [24]. The presence of residual spectral weight at  $E_F$  might be connected to this discrepancy [10], but further theoretical work is needed to clarify this issue.

An alternative explanation is that in LSCO there is a critical doping point below which the superconducting gap function changes from  $d_{x^2-y^2}$  to another form. The pseudogap at  $T > T_c$  is a precursor to superconductivity which has similar momentum dependence and amplitude as the superconducting gap [25,26]. By considering all the possible nodeless pure and mixed gap functions [2,27], we find that the combination of  $d_{x^2-y^2} + id_{xy}$  gaps is the only form that can reproduce the momentum dependence of the measured gap function quantitatively. In Fig. 3(e) we plot  $\Delta(\mathbf{k}) = |\Delta_{d_{x^2-y^2}}(\mathbf{k}) + i\Delta_{d_{xy}}(\mathbf{k})|$ , as a function of FS angle ( $\phi$ ), where  $\Delta_{d_{xy}}(\mathbf{k}) = \Delta_{d_{xy}}^0 [\sin(k_x a) \sin(k_y a)]$ . We take  $\Delta_{d_{x^2-y^2}}^0 = 1.07\Delta_{\text{antinode}}$  and  $\Delta_{d_{xy}}^0 = \Delta_{\text{diag}}$ , where  $\Delta_{\text{antinode}}$  and  $\Delta_{\text{diag}}$  are the measured gap sizes at the zone boundary and the zone diagonal, respectively. The prefactor of 1.07 comes from  $2/[\cos(k_{Fx}a) - \cos(k_{Fy}a)]$ , where  $(k_{Fx}, k_{Fy})$  is the intersection of the FS and the zone boundary. Remarkably, excellent agreement is found between the experimental data and the mixed  $d_{x^2-y^2} + id_{xy}$  gap

function along the entire FS for all the temperatures. To see this, we simply hold  $\Delta_{d_{x^2-y^2}}^0$  constant and use the measured gap sizes on the zone diagonal ( $\Delta_{\text{diag}}$ ) for the amplitude of the  $d_{xy}$  contribution to the mixed  $d_{x^2-y^2} + id_{xy}$  gap at different temperatures. The results are shown in comparison to the data in Fig. 3(e). Interestingly, the mixed  $d_{x^2-y^2} + id_{xy}$  pair state implies that the time-reversal symmetry is broken in the system [2], which has been embodied in early theories of quantum phase transitions [28].

To summarize, our main experimental findings are (1) for highly underdoped LSCO ( $x = 0.08$ ), in the superconducting state the electronic excitations are gapped along the entire underlying FS, (2) the diagonal gap persists above  $T_c$  while increasing the temperature and/or reducing the hole concentration, (3) whereas the gap size on zone boundary remains constant up to 150 K, the diagonal gap is temperature dependent, and (4) at high temperature a Fermi arc emerges and its length increases with temperature. Our observations in highly underdoped LSCO could be explained either by a strong fluctuating order competing with the superconducting order parameter [17] or by a mixed  $d_{x^2-y^2} + id_{xy}$  gap function occurring when the doping is below a quantum critical point [28]. The entirely gapped Fermi surface in highly underdoped LSCO is a profound departure from the  $d_{x^2-y^2}$  form observed at moderate to high doping. Further investigations of the origins of this nodeless gap function promise to shed light on how superconductivity emerges from the Mott insulating state in high- $T_c$  cuprates.

We thank M. R. Norman, T. M. Rice, M. Sgrist, and C. Bernhard for useful discussions. This work was supported by the Swiss National Science Foundation (through MaNEP, Grant No. 200020-105151) and by the Israeli Science Foundation. We thank the beam line staff of X09LA at the SLS for their excellent support.

*Note added.*—Recently, another paper appeared reporting a diagonal gap in underdoped  $\text{Bi}_2\text{Sr}_2\text{CaCu}_2\text{O}_{8+\delta}$  above and below  $T_c$  [29]. The value of the gap observed there is  $\sim 17$  meV when  $T_c \sim 22$  K, which is indeed very close to the value we obtained in LSCO  $x = 0.08$  ( $T_c = 20$  K,  $\Delta \sim 20$  meV).

- 
- [1] A. Damascelli, Z. Hussain, and Z.-X. Shen, *Rev. Mod. Phys.* **75**, 473 (2003).
  - [2] C. C. Tsuei and J. R. Kirtley, *Rev. Mod. Phys.* **72**, 969 (2000).
  - [3] M. Månsson *et al.*, *Rev. Sci. Instrum.* **78**, 076103 (2007).
  - [4] H. B. Yang, J. D. Rameau, P. D. Johnson, T. Valla, A. Tsvelik, and G. D. Gu, *Nature (London)* **456**, 77 (2008).
  - [5] M. Shi *et al.*, *Phys. Rev. Lett.* **101**, 047002 (2008).
  - [6] M. Shi *et al.*, *Europhys. Lett.* **88**, 27008 (2009).
  - [7] M. R. Norman *et al.*, *Nature (London)* **392**, 157 (1998).
  - [8] A. Kanigel *et al.*, *Nat. Phys.* **2**, 447 (2006).
  - [9] T. Yoshida *et al.*, *Phys. Rev. Lett.* **103**, 037004 (2009).

- [10] T.J. Reber *et al.*, *Nat. Phys.* **8**, 606 (2012).
- [11] Y.-B. Huang, P. Richard, X.-P. Wang, T. Qian, and H. Ding, [arXiv:1208.4717](https://arxiv.org/abs/1208.4717).
- [12] W. S. Lee, I. M. Vishik, K. Tanaka, D. H. Lu, T. Sasagawa, N. Nagaosa, T. P. Devereaux, Z. Hussain, and Z.-X. Shen, *Nature (London)* **450**, 81 (2007).
- [13] K. M. Shen *et al.*, *Phys. Rev. B* **69**, 054503 (2004).
- [14] Z.-H. Pan *et al.*, *Phys. Rev. B* **79**, 092507 (2009).
- [15] N. Doiron-Leyraud and L. Taillefer, *Physica (Amsterdam)* **481C**, 161 (2012).
- [16] S. Sachdev, *Physica (Amsterdam)* **470C**, S4 (2010).
- [17] W. A. Atkinson, J. D. Bazak, and B. M. Andersen, *Phys. Rev. Lett.* **109**, 267004 (2012).
- [18] B. M. Andersen, P. J. Hirschfeld, A. P. Kampf, and M. Schmid, *Phys. Rev. Lett.* **99**, 147002 (2007).
- [19] B. M. Andersen, S. Graser, and P. J. Hirschfeld, *Phys. Rev. Lett.* **105**, 147002 (2010).
- [20] G. S. Boebinger, Y. Ando, A. Passner, T. Kimura, M. Okuya, J. Shimoyama, K. Kishio, K. Tamasaku, N. Ichikawa, and S. Uchida, *Phys. Rev. Lett.* **77**, 5417 (1996).
- [21] M. Sutherland *et al.*, *Phys. Rev. Lett.* **94**, 147004 (2005).
- [22] B. Lake *et al.*, *Nature (London)* **415**, 299 (2002).
- [23] K. Takenaka, J. Nohara, R. Shiozaki, and S. Sugai, *Phys. Rev. B* **68**, 134501 (2003).
- [24] Y. Ando, A. N. Lavrov, S. Komiya, K. Segawa, and X. F. Sun, *Phys. Rev. Lett.* **87**, 017001 (2001).
- [25] V. J. Emery and S. A. Kivelson, *Nature (London)* **374**, 434 (1995).
- [26] M. Randeria, N. Trivedi, A. Moreo, and R. T. Scalettar, *Phys. Rev. Lett.* **69**, 2001 (1992).
- [27] J. F. Annet, *Adv. Phys.* **39**, 83 (1990).
- [28] M. Vojta, Y. Zhang, and S. Sachdev, *Phys. Rev. Lett.* **85**, 4940 (2000).
- [29] I. M. Vishik *et al.*, *Proc. Natl. Acad. Sci. U.S.A.* **109**, 18332 (2012).